Photoluminescence of erbium-doped silicon: excitation power dependence

© C.A.J. Ammerlaan, D.T.X. Thao, T. Gregorkiewicz, N.A. Sobolev*

Van der Waals-Zeeman Institute, University of Amsterdam,
Valckenierstraat 65, NL–1018 XE Amsterdam, The Netherlands
* A.F. Ioffe Physicotechnical Institute, Russian Academy of Sciences,
194021 St.Petersburg, Russia

(Получена 19 января 1999 г. Принята к печати 20 января 1999 г.)

The intensity of the photoluminescence of erbium in silicon is analysed by a model which takes into account the formation of free excitons, the binding of excitons to erbium ions, the excitation of inner-shell $4f$ electrons of erbium ions and their subsequent decay by light emission. Predictions of this model for the dependence of luminescence intensity on laser excitation power are compared with experimental observations. The results for float-zone and Czochralski-grown silicon in which erbium is introduced by implantation with or without oxygen co-implantation are remarkably similar. To obtain agreement between model analysis and experimental data it is necessary to include in the model terms describing energy dissipation by an Auger process of both the erbium-bound excitons and the erbium ions in excited state with free electrons in the conduction band. A good quantitative agreement is achieved.

1. Introduction

The phenomenon of luminescence of rare-earth doped semiconductors is presently under intense study. In the more fundamentally oriented research, the complex physical processes active in energy transfer from excitation in the entrance channel to light emission in the output channel are investigated. Stimulated by the perspective of practical application of this light source, erbium in silicon, emitting at wavelength of $1.54\,\mu$m, is a prominent system. In a currently accepted model energy fed into the system leads to light emission by erbium ions in a multi-step process. Radiation incident on the silicon, with photon energy larger than its bandgap, creates free electrons and holes. Free carriers combine into excitons which can be trapped at the erbium ions. The energy of erbium-bound excitons is transferred to erbium ions and results in excitation of $4f$ core electrons from the $^4I_{15/2}$ ground state into the $^4I_{13/2}$ excited state. Upon decay of excited erbium ions the characteristic luminescence is produced. In the present report this chain of processes is analysed in a mathematical model with an aim of achieving a quantitative description.

2. Photoluminescence model

2a. Energy transfer without Auger processes

The physical model as mentioned above, that will be considered in this paper, is illustrated in Fig. 1. In a recent paper by Bresler and co-workers the model, however without the Auger processes, has been put on a mathematical basis [1]. A set of rate equations was formulated for free electrons, with concentration n, free excitons, concentration n_x, erbium-bound excitons, concentration n_{xb} and erbium ions in excited state, concentration n^*_{Er}. The steady state is described by the balance equations (1) to (4), to be discussed as follows.

The chain of processes leading to photoluminescence has as the first step the generation of free electrons and holes, to equal concentrations, with rate G by the incident light. Free carriers can combine in a second-order process with rate $\gamma_x n^2$ into free excitons. Trapping of the excitons at erbium sites will be proportional to both the concentrations of the free excitons and the available free erbium sites. The latter concentration is given as the total concentration of erbium n_{Er} multiplied by the fraction of free sites $[(n_{\mathrm{Er}} - n_{xb})/n_{\mathrm{Er}}]$. Energy will be transferred to erbium $4f$ core electrons with a transfer time τ^* but again only to the erbium ions still available in their ground state, i.e. to the fraction $[(n_{\mathrm{Er}} - n^*_{\mathrm{Er}})/n_{\mathrm{Er}}]$. At high excitation power these fractions given between square brackets will tend to zero and lead to saturation of luminescence output. This manifestation of saturation is related to exhaustion of available erbium centres. Finally, luminescence is produced by the decay with time constant τ_d of erbium ions n^*_{Er} in the excited state. The photon emission rate equal to n^*_{Er}/τ_d is the quantity measured in the experiment.

Reverse processes as indicated in Fig. 1 by arrows pointing to the left, are thermally activated. They include the dissociation of excitons into free electrons and holes fn_x requiring energy gain of E_x, the release of excitons from erbium trapping sites cfn_{xb}, and a back transfer process in which an erbium-bound exciton is recreated from an excited erbium ion. Though these reverse processes hamper the energy transfer towards light emission, they do not remove energy from the chain. The coefficients of forward and reverse processes are related by considerations of detailed balancing.

Energy is permanently lost by processes which remove energy irreversibly from the chain. Such processes, as indicated in Fig. 1 by vertical arrows downwards, are recombination of electrons and holes via other centres, with rate γn^2, and recombination of free excitons directly or via alternative centres, n_x/τ_x. The Auger processes represented in Fig. 1 also remove energy from the luminescence path irreversibly.

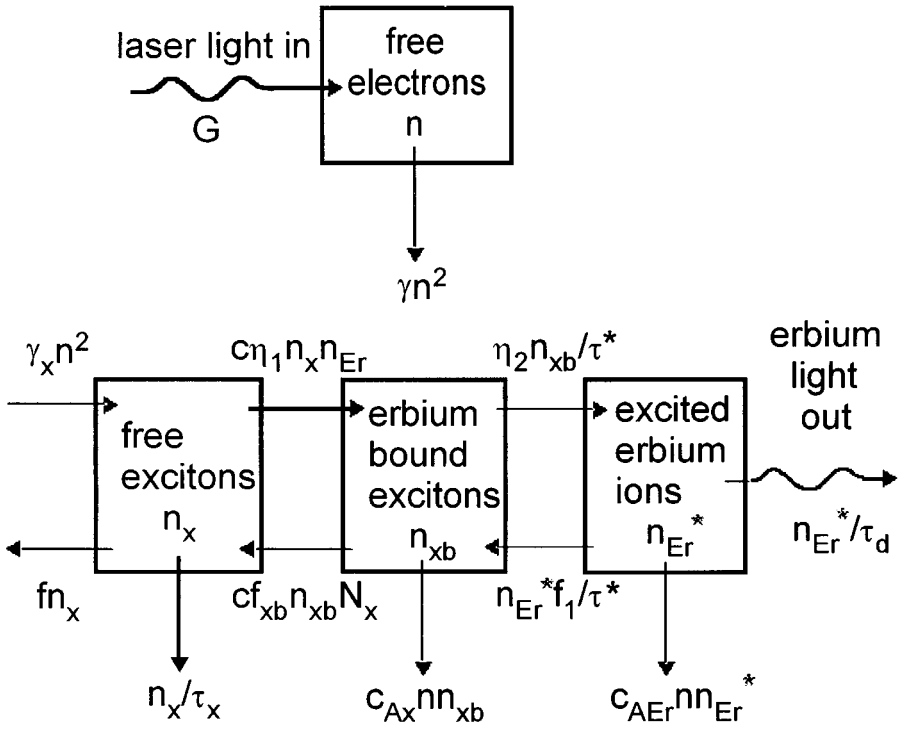

Figure 1. Two stream-model for the photo-excitation of erbium luminescence showing generation and loss of free electrons n, free excitons n_x, erbium-bound excitons n_{xb} and erbium ions in excited state n^*_{Er}. Notation: $\eta_1 = (n_{Er} - n_{xb})/n_{Er}$, $\eta_2 = (n_{Er} - n^*_{Er})/n_{Er}$.

Balance equations based on these processes are

$$G + fn_x = \gamma n^2 + \gamma_x n^2, \tag{1}$$

$$\gamma_x n^2 + cf_{xb} n_{xb} N_x = cn_x n_{\mathrm{Er}}\left[(n_{\mathrm{Er}} - n_{xb})/n_{\mathrm{Er}}\right] + fn_x + n_x/\tau_x, \tag{2}$$

$$cn_x n_{\mathrm{Er}}\left[(n_{\mathrm{Er}} - n_{xb})/n_{\mathrm{Er}}\right] + n^*_{\mathrm{Er}} f_1/\tau^* = n_{xb}\left[(n_{\mathrm{Er}} - n^*_{\mathrm{Er}})/n_{\mathrm{Er}}\right]/\tau^* + cf_{xb} n_{xb} N_x, \tag{3}$$

and

$$n_{xb}\left[(n_{\mathrm{Er}} - n^*_{\mathrm{Er}})/n_{\mathrm{Er}}\right]/\tau^* = n^*_{\mathrm{Er}}/\tau_d + n^*_{\mathrm{Er}} f_1/\tau^*. \tag{4}$$

Generation terms are given on the left hand sides of these equations; loss terms appear in each case on the right hand side. An exact solution for the equations, in the form of a quadratic equation for n^*_{Er}, is presented by Bresler, et al. [1]. The result takes a more simplified form by the restriction to low temperatures, e. g., liquid-helium temperature, when all reverse processes, which require thermal activation, are suppressed. Under these conditions, when $f = f_{xb} = f_1 = 0$, one obtains

$$a_0\left(n^*_{\mathrm{Er}}/n_{\mathrm{Er}}\right)^2 - \left(b_0 + b_2 G\right)\left(n^*_{\mathrm{Er}}/n_{\mathrm{Er}}\right) + c_2 G = 0, \tag{5}$$

with

$$a_0 = 1 + cn_{\mathrm{Er}}\tau_x\left[1 + (\tau^*/\tau_d)\right], \tag{5a}$$

$$b_0 = 1 + cn_{\mathrm{Er}}\tau_x, \tag{5b}$$

$$b_2 = \gamma_x \tau_x c\tau_d\left[1 + (\tau^*/\tau_d)\right]/\gamma, \tag{5c}$$

and

$$c_2 = \gamma_x \tau_x c\tau_d/\gamma. \tag{5d}$$

In its general form, the equation predicts saturation of n^*_{Er} at the level $n^*_{\mathrm{Er}}/n_{\mathrm{Er}} = c_2/b_2$ for high excitation power G. For low power a linear relationship $n^*_{\mathrm{Er}}/n_{\mathrm{Er}} = (c_2/b_0)G$ is predicted. In comparing experimental data with these model equations one must be aware that neither generation power nor output luminescence are known very well in absolute numbers. For instance the volume in the sample where excitation takes place is not well defined. For this reason it is of advantage to eliminate these uncertain factors by resorting to relative units. As regards luminescence intensity the obvious unit for normalization is the saturation value c_2/b_2. A dimensionless normalized intensity is therefore introduced as $I \equiv (n^*_{\mathrm{Er}}/n_{\mathrm{Er}})/(c_2/b_2)$. For the excitation power the unit is obtained as the value at which the extrapolated linear increase at low power crosses the saturation level. This will be at $G_1 = b_0/b_2$. The normalized power $P \equiv G/G_1$ is again a dimensionless quantity. In terms of normalized units equation (5) is modified into

$$I^2 - \alpha(1 + P)I + \alpha P = 0, \tag{6}$$

with

$$\alpha \equiv b_0 b_2/a_0 c_2. \tag{6a}$$

It turns out that the dependence of intensity I on generation power P is governed by one parameter α, through which

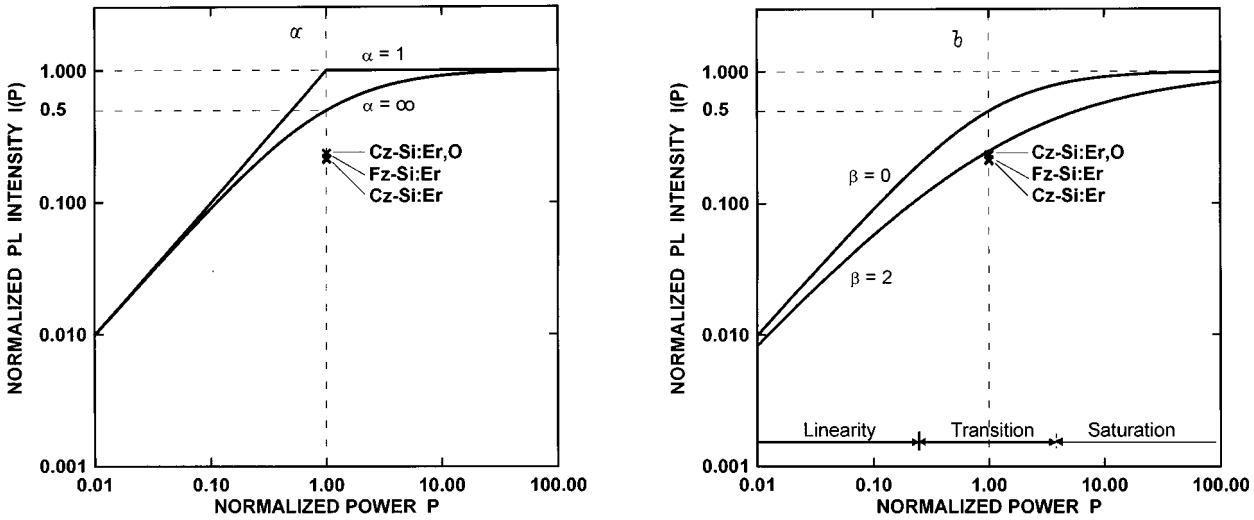

Figure 2. Dependence of normalized luminescence output I as a function of normalized laser power input P; *a*) for the model without Auger processes, *b*) for a model including strong Auger decay processes. Experimental data for three samples of type *Fz*-Si : Er, *Cz*-Si : Er and *Cz*-Si : Er,O are given for unit power $P = 1$.

the specific aspects of the luminescence process as a whole are represented. However, from equation (6) it is easily concluded that for low power $I = P$, and for high power $I = 1$, irrespective the value of the parameter α. In normalized form the parameters a_2, b_0, b_2 and c_2, or in basic more physical form γ, γ_x, c, τ_x, τ^* and τ_d, have no effect on the power dependence in the low and high power regions. Only at intermediate power, i. e., at $P \approx 1$, the results will depend on α. Only in the transition region from linear increase to saturation the observed luminescence does reveal insight into the luminescence process. The most typical value to study the luminescence mechanism is therefore at power $P = 1$. At this level the luminescence intensity is given by

$$I = \alpha - (\alpha^2 - \alpha)^{1/2}. \tag{7}$$

From the equality $\alpha = b_0 b_2 / a_0 c_2$ and the parameters as given by equations (5a–d) one concludes that $1 \leqslant \alpha \leqslant \infty$. For such values of α always solutions from equation (7) do exist. For $\alpha = 1$ one obtains $I(P = 1) = 1$ and for $\alpha = \infty$ one has $I(P = 1) = 0.5$. The range of possible luminescence intensities at unit power $P = 1$ consistent with equation (6) is restricted between 0.5 and 1. The limiting curves for an extended power range are drawn in Fig. 2, *a*.

In Fig. 2, *a* also experimental data are included. They result from measurements at liquid helium temperature on three samples with different specifications. The sample *Fz*-Si : Er is float zoned silicon implanted with erbium. Sample labelled *Cz*-Si : Er is Czochralski silicon similarly implanted. The third sample, labelled *Cz*-Si : Er,O was co-doped with oxygen by implantation. In all cases the luminescence intensity was followed as a function of excitation power. Experimental data are plotted for normalized power $P = 1$ at the observed values $I \approx 0.22$. Obviously, this is outside the range of results as can be described by the model.

2b. Energy transfer with Auger processes

One has to conclude that the presented model is unable to provide the quantitative description of the luminescence process. In order to improve the model energy losses through Auger processes may be considered, as has been explored before by Palm et al. [2]. Erbium-bound excitons can dissipate their energy in an Auger process with involvement of free electrons. Similarly, erbium ions in excited state can decay in an Auger process, also with conduction band electrons. These processes are as well indicated in Fig. 1. In the balance equations they are implemented by including on the loss side the Auger rates $c_{Ax} n n_{xb}$ and $c_{AEr} n n^*_{Er}$. The extended balance equations for bound excitons and excited erbium ions become

$$c n_x n_{Er} \left[(n_{Er} - n_{xb}) / n_{Er} \right] + n^*_{Er} f_1 / \tau^* = n_{xb} \left[(n_{Er} - n^*_{Er}) / n_{Er} \right] / \tau^* + c f_{xb} n_{xb} N_x + c_{Ax} n n_{xb}, \tag{8}$$

and

$$n_{xb} \left[(n_{Er} - n^*_{Er}) / n_{Er} \right] / \tau^* = n^*_{Er} / \tau_d + n^*_{Er} f_1 / \tau^* + c_{AEr} n n^*_{Er}. \tag{9}$$

In order to solve the new set of equations (1), (2), (8) and (9) it is helpful to introduce appropriate simplifications. Considering numerical values one may conclude that the loss of free electrons and holes is dominated by their recombination via traps with rate γn^2. The loss via exciton formation $\gamma_x n^2$ is comparatively much less, i. e., $\gamma_x \ll \gamma$. Under such conditions the energy transfer model can be cascaded into two parts. In stream I the balance of electrons is considered separately by equation (1). The loss of electrons through exciton formation is ignored in this

mainstream. At low temperature this leads to

$$G = \gamma n^2, \tag{10}$$

$$n = (G/\gamma)^{1/2}. \tag{11}$$

The electron concentration obtained via this solution is used to describe the Auger processes. Typical numbers are $G = 10^{22}\,\mathrm{cm^{-3}s^{-1}}$, $\gamma = 10^{-10}\,\mathrm{cm^3s^{-1}}$ and $n = 10^{16}\,\mathrm{cm^{-3}}$.

In energy stream II the balance of free excitons, bound excitons and excited erbium ions is separately considered. Solution of the equations leads to a cubic equation in $n^*_{\mathrm{Er}}/n_{\mathrm{Er}}$, which, accepting some approximation, can be factorized to yield a quadratic equation

$$\begin{aligned}&\left(a_0 + a_1 G^{1/2} + a_2 G\right)\left(n^*_{\mathrm{Er}}/n_{\mathrm{Er}}\right)^2 \\ &\quad - \left(b_0 + b_1 G^{1/2} + b_2 G + b_3 G^{3/2}\right)\left(n^*_{\mathrm{Er}}/n_{\mathrm{Er}}\right) \\ &\quad + c_2 G = 0,\end{aligned} \tag{12}$$

with

$$a_0 = 1 + cn_{\mathrm{Er}}\tau_x\left[1 + (\tau^*/\tau_d)\right], \tag{12a}$$

$$\begin{aligned}a_1 = \big[&(1 + cn_{\mathrm{Er}}\tau_x)c_{A\mathrm{Er}}\tau_d \\ &+ 2cn_{\mathrm{Er}}\tau_x(\tau^*/\tau_d)c_{A\mathrm{Er}}\tau_d\big]/\gamma^{1/2},\end{aligned} \tag{12b}$$

$$a_2 = cn_{\mathrm{Er}}\tau_x(\tau^*/\tau_d)(c_{A\mathrm{Er}}\tau_d)^2/\gamma, \tag{12c}$$

$$b_0 = 1 + cn_{\mathrm{Er}}\tau_x, \tag{12d}$$

$$b_1 = (1 + cn_{\mathrm{Er}}\tau_x)(c_{A\mathrm{Er}}\tau_d + c_{Ax}\tau^*)/\gamma^{1/2}, \tag{12e}$$

$$\begin{aligned}b_2 = \Big\{&(1 + cn_{\mathrm{Er}}\tau_x)c_{A\mathrm{Er}}\tau_d c_{Ax}\tau^* \\ &+ \gamma_x\tau_x c\tau_d\left[1 + (\tau^*/\tau_d)\right]\Big\}/\gamma,\end{aligned} \tag{12f}$$

$$b_3 = \gamma_x\tau_x c\tau_d c_{A\mathrm{Er}}\tau_d(\tau^*/\tau_d)/\gamma^{3/2}, \tag{12g}$$

and

$$c_2 = \gamma_x\tau_x c\tau_d/\gamma. \tag{12h}$$

At low power the model equatioans reflect the linear increase $n^*_{\mathrm{Er}}/n_{\mathrm{Er}} = (c_2/b_0)G$, just as before. At high power, however, the consistent solution $n^*_{\mathrm{Er}}/n_{\mathrm{Er}} = (c_2/b_3)/G^{1/2}$ predicts decreasing luminescence intensity upon increase of the excitation source. Such behaviour is to be expected as in the present case two independent saturation mechanisms are active. The first one drives the concentration of erbium-bound excitons, n_{xb}, towards the concentration of available erbium ions but is limited to stay below or become equal to this concentration. The second saturation mechanism is the combined action of the two Auger processes. At high power, and hence high concentrations of free electrons, the Auger mechanism removing excited erbium ions nonradiatively becomes very effective. This will result in a reduction of n^*_{Er}, which becomes proportional to $1/n$, or $1/G^{1/2}$. Such a decrease has not been observed in the present experiments; it has also not been reported in the literature. Inspection of the equations shows that one should expect the decrease to set in at excitation values where $c_{A\mathrm{Er}}\tau_d(\tau^*/\tau_d)(G/\gamma)^{1/2} > 1$. Considering numerical values ($c_{A\mathrm{Er}} \approx 10^{-12}\,\mathrm{cm^3}\cdot\mathrm{s^{-1}}$, $\tau^* \approx 10^{-6}\,\mathrm{s}$) this corresponds to high values of G, near and above $10^{26}\,\mathrm{cm^{-3}}\cdot\mathrm{s^{-1}}$, which are not reached in actual experiments. This can be attributed to the small value of (τ^*/τ_d), as τ^* is in the range of microseconds and τ_d is of order milliseconds. Introducing the approximation $\tau^*/\tau_d \approx 0$, equations (12) reduce in many respects to equations (6). In particular the term $b_3G^{3/2}$ in equation (12) is lost and the equation predicts saturation at c_2/b_2.

Both for low and for high power the solution of equation (12) will be

$$n^*_{\mathrm{Er}}/n_{\mathrm{Er}} = c_2G/(b_0 + b_1G^{1/2} + b_2G). \tag{13}$$

This result will also be valid for intermediate power in case the Auger processes are strong. Following solution (13) one has saturation at c_2/b_2, linear increase at low power with $(c_2/b_0)G$, and $G_1 = b_0/b_2$. Casting equation (13) in terms of normalized units, as before, the result will read

$$I = P/(1 + \beta P^{1/2} + P) \tag{14}$$

with

$$\beta = b_1/(b_0b_2)^{1/2}, \tag{14a}$$

or

$$\begin{aligned}\beta = \left(c_{A\mathrm{Er}}\tau_d + c_{Ax}\tau^*\right)/\big[&c_{A\mathrm{Er}}\tau_d c_{Ax}\tau^* \\ &+ \gamma_x\tau_x c\tau_d/(1 + cn_{\mathrm{Er}}\tau_x)\big]^{1/2}.\end{aligned} \tag{14b}$$

Under the assumed condition of strong Auger effect this reduces to

$$\beta = \left(c_{A\mathrm{Er}}\tau_d + c_{Ax}\tau^*\right)/\left(c_{A\mathrm{Er}}\tau_d c_{Ax}\tau^*\right)^{1/2}, \tag{14c}$$

or

$$\beta = \left(c_{A\mathrm{Er}}\tau_d/c_{Ax}\tau^*\right)^{1/2} + \left(c_{Ax}\tau^*/c_{A\mathrm{Er}}\tau_d\right)^{1/2}. \tag{14d}$$

As usual the power dependence of the luminescence has its linear increase at low power with $I = P$ and saturates at high power at $I = 1$. Features of the luminescence process are only revealed at intermediate power, e.g., at $P = 1$, where $I = 1/(2 + \beta)$. For a general case parameter β will be positive following equation (14b); for the case of strong Auger effect $\beta \geqslant 2$, as follows from equations (14c,d). Fig. 2, *b* illustrates the curves as obtained from equation (14) for $\beta = 0$ and $\beta = 2$. Compared to the previous case, without Auger effect, the transition region between linear behaviour and saturation is broader. This is due to the appearance of the $P^{1/2}$ term as a consequence of the Auger effect.

Considering again the experiment, the measured data for the luminescence power dependence for sample *Cz*-Si : Er,O are plotted in Fig. 3. The solid curve is the best fit using equation (14) with parameter $\beta = 2.25$. Similar fits were also made for the samples *Fz*-Si : Er and *Cz*-Si : Er,

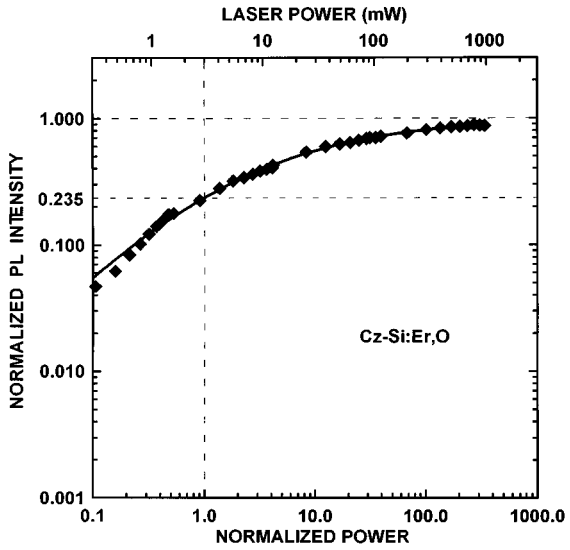

Figure 3. Photoluminescence intensity, in normalized units I, as a function of applied laser excitation power, both in units G of laser power and in normalized units P for the sample Cz-Si : Er,O. Experimental data points and theoretical curve according to formula (14) with parameter $\beta = 2.25$.

the parameter values are then $\beta = 2.63$ and 2.73, respectively [3]. The data points for the three samples for $P = 1$ and $I = 1/(2 + \beta)$ are also plotted in Fig. 2, *b*. The results for the three samples are quite similar with $\beta = 2.5 \pm 0.25$. With equation (14d) the result is converted to $(c_{AEr}\tau_d / c_{Ax}\tau^*)^{\pm 1} \approx (4 \pm 1)$. This compares favourably with data as published in the literature, e. g., $c_{AEr} = 10^{-12}\,\mathrm{cm}^3 \cdot \mathrm{s}^{-1}$, $\tau_d = 10^{-3}\,\mathrm{s}$, $c_{Ax} = 10^{-10}\,\mathrm{cm}^3 \cdot \mathrm{s}^{-1}$, and $\tau^* = 4 \cdot 10^{-6}\,\mathrm{s}$ [2]. From the present analysis one can only conclude that $c_{AEr}\tau_d / c_{Ax}\tau^*$ is very similar in the three kinds of material investigated. This can be due to an accidental combination of parameters, but one is tempted to believe that all process paramters, i. e., c_{AEr}, τ_d, c_{Ax} and τ^*, have similar values. In such case the possible difference in structure of the luminescent centres in the three materials has very little influence on the efficiency of the photoluminescence process.

The work was supported in part by the INTAS–RFBR (grant 95-0531).

References

[1] M.S. Bresler, O.B. Gusev, B.P. Zakharchenya, I.N. Yassievich. Phys. Sol. St., **38**, 813 (1996).
[2] J. Palm, F. Gan, B. Zheng, J. Michel, L.C. Kimerling. Phys. Rev. B, **54**, 17 603 (1996).
[3] D.T.X. Thao, et al. (to be published).

Редактор В.В. Чалдышев